第 6 卷 第 3 期 航空动力学报 Vol. 6 No. 3
1991 年 7 月 Journal of Aerospace Power July 1991

无定心弹簧刚性转子—SFDB 系统非同步稳态响应的稳定性分析*

西北工业大学 张嘉欣** 薛中擎

【摘要】 本文用谐波平衡法研究了无定心弹簧刚性转子—挤压油膜阻尼器轴承 (SFDB) 系统的稳态响应和稳定性，其中通过二个耦合的二阶微分方程来近似模拟运动，非线性油膜力作用处的非同步稳态响应通过运动微分方程的周期解求得。本文建立了油膜力的等效线性化模型。提出了新的稳定性分析方法。利用导出的等效动力特性系数建立了稳定性分析的判据，证明满足此判据的稳态响应是稳定的。并以该系统的次谐波响应为例，比较了本方法与数值积分方法的计算结果。

一、运动方程和油膜力方程

对图 1a 所示的刚性转子—SFDB 系统，在结构对称的假设下，可以简单地将转子质量 2m

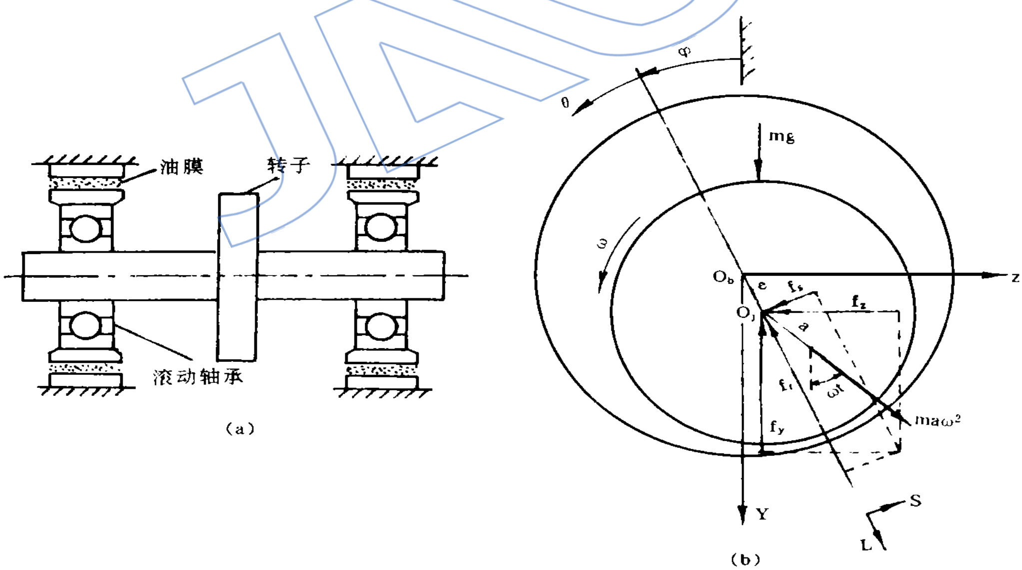

图 1 刚性转子—SFDB 系统及轴承站示意图

平分到两端轴承站上，于是只需考察单个轴承站上的运动即可。由图 1b 可见，油膜分力在固定坐标系上为 f_x 和 f_y，在旋转坐标系上为 f_r 和 f_s。因此可写出转子在 yoz 的运动微分方程:

$$m\ddot{y} = mg + f_y + ma\omega^2\cos\omega t \quad , \quad m\ddot{z} = f_z + ma\omega^2\sin\omega t \tag{1}$$

本文于 1990 年 3 月收到。 ** 西安市西北工业大学 378 信箱 710072

式中f_y 和f_z 与f_r 和f_s 间的关系为

$$f_y = -(f_r\cos\varphi - f_s\sin\varphi)\quad,\quad f_z = -(f_r\sin\varphi + f_s\cos\varphi) \tag{2}$$

而f_r 和f_s 不难用短轴承近似理论及 π 油膜空穴边界条件从 Reynolds 方程求出:

$$f_r = -(\eta RL^3/c^2)(\dot{\varepsilon}I_3^{02} + \varepsilon\dot{\varphi}I_3^{11})\quad,\quad f_s = -(\eta RL^3/c^2)(\dot{\varepsilon}I_3^{11} + \varepsilon\dot{\varphi}I_3^{20}) \tag{3}$$

式中的积分 $I_n^{lm} = \int_{\theta_1}^{\theta_2}(\sin^l\theta + \cos^m\theta)\,d\theta/(1+\varepsilon\cos\theta)^n$ 可利用 Sommerfeld 变换 $\cos\gamma = (\varepsilon + \cos\theta)/(1+\varepsilon\cos\theta)$ 或 Booker 的颈轴承表[1]求出。积分极限 $\theta_2 = \theta_1 + \pi$, $\theta_1 = \tan^{-1}(-\dot{\varepsilon}/\varepsilon\dot{\varphi})$。$\varepsilon = e/c$ 为偏心率; c 为阻尼器径向间隙; R 为轴承半径; L 为阻尼器承载长度; η 为润滑油的绝对粘度。

为了便于分析, 将式(1)无量纲化, 引入 $Y = y/c$, $Z = z/c$, $\tau = \omega t$, 重力参数 $W = g/c\omega^2$, 轴承参数 $B = \eta RL^3/m\omega c^3$, 不平衡参数 $U = a/c$, 令 $' = d/d\tau$, $'' = d^2/d\tau^2$, 则式(1)改写成

$$Y'' = W + F_y + U\cos\tau\quad,\quad Z'' = F_z + U\sin\tau \tag{4}$$

式中 F_y 和 F_z 为无量纲油膜力

$$\begin{aligned} F_y &= B[(\varepsilon' I_3^{02} + \varepsilon\varphi' I_3^{11})\cos\varphi - (\varepsilon' I_3^{11} + \varepsilon\varphi' I_3^{20})\sin\varphi] = BF_1 \\ F_z &= B[(\varepsilon' I_3^{02} + \varepsilon\varphi' I_3^{11})\sin\varphi - (\varepsilon' I_3^{11} + \varepsilon\varphi' I_3^{20})\cos\varphi] = BF_2 \end{aligned} \tag{5}$$

这里显然有以下关系 $\varepsilon = \sqrt{Y^2 + Z^2}$, $\cos\varphi = Y/\varepsilon$, $\sin\varphi = Z/\varepsilon$

$$\varepsilon' = Y'\cos\varphi + Z'\sin\varphi\quad,\quad \varepsilon\varphi' = -Y'\sin\varphi + Z'\cos\varphi$$

$$\therefore\quad F_i = F_i(Y, Z, Y', Z')\qquad (i = 1, 2) \tag{6}$$

二、非同步稳态响应

无量纲方程(4)表示一个扰频 $\bar{\omega} = 1$, 周期 $T = 2\pi$ 的谐和力所激励的系统。由于油膜力的非线性, 这个系统将产生非同步(一般是次谐波)共振[2], 即振动频率 Ω 与激励频率 $\bar{\omega}$ 不同步的振动, 其关系为 $\Omega = (n/N)\bar{\omega}$, 其中 n、N 是互为素数的正整数, 且 $N > n$。大家知道, 任何周期函数都可以表示为正弦和余弦分量的傅里叶级数。设方程(4)具有周期为 $2\pi/\Omega$ 的周期解 $Y(\tau)$、$Z(\tau)$, 可表示为

$$\begin{aligned} Y(\tau) &= a_{10} + \sum_{j=1}^{N}[a_{1j}\cos(jn\tau/N) + b_{1j}\sin(jn\tau/N)] \\ Z(\tau) &= a_{20} + \sum_{j=1}^{N}[a_{2j}\cos(jn\tau/N) + b_{2j}\sin(jn\tau/N)] \end{aligned} \tag{7}$$

上式在物理上表示强迫振动非线性系统的非同步稳态响应轨迹[3,4,5]。其中各谐波系数 a_{io}、a_{ij}、b_{ij} ($i = 1, 2$; $j = 1, 2, \cdots, N$) 都是待定常数。当 $n = N = 1$ 时, 式(7)表示基频为 1、加谐波的谐波响应。当 $n = 1$, $N \geqslant 2$ 时, 式(7)表示基频为 $1/N$ 的 $1/N$ 阶次谐波响应; 当 n, $N \geqslant 2$, 且 n/N, $n/N \neq 1, 2, \cdots$ 时, 则表示基频为 n/N 阶超次谐波响应。

将式(7)代入式(6), 可知 F_1、F_2 也是周期函数, 可用另一傅里叶级数来表示:

$$\begin{aligned} F_1(\bar{\tau}) &= A_{10} + \sum_{j=1}^{N}(A_{1j}\cos j\bar{\tau} + B_{1j}\sin j\bar{\tau}) \\ F_2(\bar{\tau}) &= A_{20} + \sum_{j=1}^{N}(A_{2j}\cos j\bar{\tau} + B_{2j}\sin j\bar{\tau}) \end{aligned} \tag{8}$$

式中 $\bar{\tau}=(n/N)\tau$, $A_{io}=\frac{1}{2\pi}\int_o^{2\pi}F_i(\bar{\tau})d\bar{\tau}$, $A_{ij}=\frac{1}{2\pi}\int_o^{2n}F_i(\bar{\tau})\cos j\bar{\tau}d\bar{\tau}$, $B_{ij}=\frac{1}{2\pi}\int_o^{2n}F_i(\bar{\tau})\sin j\bar{\tau}d\bar{\tau}$
$(i=1, 2; j=1, 2, \cdots, N)$。由式 (5) 可知, F_i 在区间 $[0, 2\pi]$ 上绝对可积, 因此系数 A_{io}、A_{ij}、B_{ij} 是确定的。

将式 (7) 和 (8) 均代入式 (4), 取其谐波平衡, 即两端同阶谐波分量的系数等同, 得:

$$
\begin{aligned}
&W+BA_{10}=0 && BA_{20}=0 \\
&a_{ij}=-(N/jn)^2BA_{ij} && b_{ij}=-(N/jn)^2BB_{ij}\quad (n=1, N\geqslant 2, j=1, 2, \cdots, N-1) \\
&a_{1N}=-BA_{1N}-U && b_{1N}=-BB_{1N} \\
&a_{2N}=-BA_{2N} && b_{2N}=-BB_{2N}-U\quad (n=1, N\geqslant 2, j=N)
\end{aligned}
\tag{9}
$$

这非线性代数方程组虽含有 $4N+2$ 个方程, 实际上只能用其中的 $4N$ 个方程来解出 $4N$ 个未知量 a_{ij}、b_{ij} $(i=1, 2; j=1, 2, \cdots, N)$。由于系数 a_{io} $(i=1, 2)$ 尚为未知, 所以要完全确定式 (7) 所假设的稳态响应轨迹, 还得通过一定迭代步骤来求解。

三、等效动力特性系数

有了确定的运动轨道, 就可建立相应的动力特性系数, 但该系统没有静平衡位置, 不能用传统的 Taylor 级数展开法。本文从等效线性化的概念出发来求这些系数。

由于油膜力的非线性, 对于不同的运动轨道, 与之对应的线性力及系数是不同的。对于形式如式 (7) 的运动轨道, 假设非线性油膜力分量 F_y 和 F_z 可线性化为

$$
\begin{aligned}
F_y &\sim F_{10}-K_{11}Y-K_{12}Z-C_{11}Y'-C_{12}Z'+\sum_{j=1}^{N}\left[P_{1j}\cos\left(\frac{jn\tau}{N}\right)+Q_{1j}\sin\left(\frac{jn\tau}{N}\right)\right] \\
F_z &\sim F_{20}-K_{21}Y-K_{22}Z-C_{21}Y'-C_{22}Z'+\sum_{j=1}^{N}\left[P_{2j}\cos\left(\frac{jn\tau}{N}\right)+Q_{2j}\sin\left(\frac{jn\tau}{N}\right)\right]
\end{aligned}
\tag{10}
$$

式中“~”号表示等效, 即符号两方力的作用都产生式 (7) 所设定的运动轨道。F_{io} $(i=1, 2)$ 是等效平均力, K_{ij} $(i, j=1, 2)$ 是油膜等效刚度系数, C_{ij} $(i, j=1, 2)$ 是油膜等效阻尼系数, 而 P_{ij} 和 Q_{ij} $(i=1, 2; j=1, 2, \cdots, N; N\geqslant 2; n=1)$ 是等效外谐和力的幅值。

$n=1$, $N\geqslant 2$ 时, 式 (7) 中对应于 $j=N$ 的项代表与外力同步的响应分量, 对应于 $j\neq N$ 的项则代表与外力不同步的响应分量。如果式 (7) 中不含 $j\neq N$ 的项, 运动将与外谐和力同步。于是式 (10) 中将不含等效外谐和力, 这表明等效线性系统中没有非同步响应分量。

将式 (10) 代入式 (4) 得

$$
\begin{aligned}
Y'' &= W+F_{10}-K_{11}Y-K_{12}Z-C_{11}Y'-C_{12}Z'+\sum_{j=1}^{N}\left[P_{1j}\cos\left(\frac{jn\tau}{N}\right)+Q_{1j}\sin\left(\frac{jn\tau}{N}\right)\right]+U\cos\tau \\
Z'' &= F_{20}-K_{21}Y-K_{22}Z-C_{21}Y'-C_{22}Z'+\sum_{j=1}^{N}\left[P_{2j}\cos\left(\frac{jn\tau}{N}\right)+Q_{2j}\sin\left(\frac{jn\tau}{N}\right)\right]+U\sin\tau
\end{aligned}
\tag{11}
$$

再将式 (7) 代入这一等效运动微分方程, 又一次应用谐波平衡法, 可得以下关系式:

$$
\begin{aligned}
&W+F_{10}-K_{11}a_{10}-K_{12}a_{20}=0 \\
&F_{20}-K_{21}a_{10}-K_{22}a_{20}=0 \\
&(jn/N)^2a_{1j}=K_{11}a_{1j}+K_{12}a_{2j}+(jn/N)C_{11}b_{1j}+(jn/N)C_{12}b_{2j}-P_{1j} \\
&(jn/N)^2b_{1j}=K_{11}b_{1j}+K_{12}b_{2j}-(jn/N)C_{11}a_{1j}-(jn/N)C_{12}a_{2j}-Q_{1j} \\
&(jn/N)^2a_{2j}=K_{21}a_{1j}+K_{22}a_{2j}+(jn/N)C_{21}b_{1j}+(jn/N)C_{22}b_{2j}-P_{2j} \\
&(jn/N)^2b_{2j}=K_{21}b_{1j}+K_{22}b_{2j}-(jn/N)C_{21}a_{1j}-(jn/N)C_{22}a_{2j}-Q_{2j}
\end{aligned}
\tag{12}
$$

式中 $n=1$; $N\geqslant 2$; $j=1, 2, \cdots, N-1$; 而当 $j=N$ 时

$$
\begin{aligned}
a_{1N} &= K_{11}a_{1N}+K_{12}a_{2N}+C_{11}b_{1N}+C_{12}b_{2N}-P_{1N}-U\\
b_{1N} &= K_{11}b_{1N}+K_{12}b_{2N}-C_{11}a_{1N}-C_{12}a_{2N}-Q_{1N}\\
a_{2N} &= K_{21}a_{1N}+K_{22}a_{2N}+C_{21}b_{1N}+C_{22}b_{2N}-P_{2N}\\
b_{2N} &= K_{21}b_{1N}+K_{22}b_{2N}-C_{21}a_{1N}-C_{22}a_{2N}-Q_{2N}-U\\
P_{1N} &= Q_{1N}=P_{2N}=Q_{2N}=0
\end{aligned}
\tag{13}
$$

式 (12) 和 (13) 共有方程 $4N+6$ 个，而待求的等效动力特性系数则为 $4N+10$ 个，可见未知数多于方程个数，解不唯一。为了使解有唯一性，必须对等效力的形式进一步加以限制。通常可以认为：①$F_{10}=F_{20}=0$，因为平均的油膜力并没有实际的物理意义；②$C_{12}=C_{21}$，因为根据轴颈轴承的研究成果，阻尼系数一般是对称的；③$K_{12}=K_{21}$，可与通常结构分析中刚度阵对称的现象保持一致。有了这些假设，便可求得等效线性系统的全部等效动力特性系数。例如，由式 (12) 的头二式和式 (13)，可先解出 K_{ij}、C_{ij} $(i, j=1, 2)$，再由式 (12) 的后四式解出 P_{ij}、Q_{ij} $(i=1, 2; j=1, 2, \cdots, N-1)$。这些等效动力特性系数均表为轨道参数 a_{io}、a_{ij}、b_{ij} $(i=1, 2; j=1, 2, \cdots, N)$ 的函数。对应于不同的运动轨道会有不同的等效动力特性系数。这一点与传统的动力特性系数在概念上不相同。

四、稳态响应的稳定性分析

式 (11) 是与运动轨道方程 (7) 相对应的等效线性运动微分方程，故可用微摄动理论来进行稳态响应的稳定性分析。对式 (11) 作等时变分，考虑到 $\Delta W=0$ 和 $\Delta U=0$，则有

$$
\begin{aligned}
\Delta Y'' =& \Delta F_{10}-K_{11}\Delta Y-Y\Delta K_{11}-K_{12}\Delta Z-Z\Delta K_{12}-C_{11}\Delta Y'-Y'\Delta C_{11}-C_{12}\Delta Z'\\
&-Z'\Delta C_{12}+\sum_{j=1}^{N}\left[\Delta P_{1j}\cos(jn\tau/N)+\Delta Q_{1j}\sin\left(\frac{jn\tau}{N}\right)\right]\\
\Delta Z'' =& \Delta F_{20}-K_{21}\Delta Y-Y\Delta K_{21}-K_{22}\Delta Z-Z\Delta K_{22}-C_{21}\Delta Y'-Y'\Delta C_{21}-C_{22}\Delta Z'\\
&-Z'\Delta C_{22}+\sum_{j=1}^{N}\left[\Delta P_{2j}\cos(jn\tau/N)+\Delta Q_{2j}\sin(jn\tau/N)\right]
\end{aligned}
\tag{14}
$$

式中 ΔY、ΔZ 是轨道的微小扰动。由于动力系数随着轨道变化，所以 ΔK_{ij}、ΔC_{ij}、ΔP_{ij}、ΔQ_{ij} $(i, j=1, 2)$ 均不为零；因已设 $F_{10}=F_{20}=0$，故 $\Delta F_{10}=\Delta F_{20}=0$。

要想直接从式 (14) 分析 ΔY 和 ΔZ 的变化情况是很困难的。为了使分析简化，可对 ΔY 和 ΔZ 进行如下变换，设

$$
\begin{aligned}
\Delta Y &= \Delta a_{10}+\sum_{j=1}^{N}\left\{\Delta a_{1j}\cos\left(\frac{jn\tau}{N}\right)+\Delta b_{ij}\sin\left(\frac{jn\tau}{N}\right)\right\}\\
\Delta Z &= \Delta a_{20}+\sum_{j=1}^{N}\left\{\Delta a_{2j}\cos\left(\frac{jn\tau}{N}\right)+\Delta b_{2j}\sin\left(\frac{jn\tau}{N}\right)\right\}
\end{aligned}
\tag{15}
$$

式中 Δa_{io}、Δa_{ij}、Δb_{ij} $(i=1, 2; j=1, 2, \cdots, N)$ 设均为随 τ 变化的函数，则不难证明此式是等价变换，因为当 $\tau\to\infty$ 时，方程的两端均趋近于零。

将式 (15) 和 (7) 代入式 (14)，再一次应用谐波平衡法，同时考虑到动力系数与轨道参数的关系式 (12) 和 (13) 的等时变换也成立，最后可得

$$
\Delta a_{10}''+C_{11}\Delta a_{10}'+C_{12}\Delta a_{20}'=0 \quad , \quad \Delta a_{20}''+C_{21}\Delta a_{10}'+C_{22}\Delta a_{20}'=0 \tag{16}
$$

$$
\begin{aligned}
&\Delta a''_{1j} + C_{11}\Delta a'_{1j} + (2jn/N)\Delta b'_{1j} + C_{12}\Delta a'_{2j} = 0 \\
&\Delta b''_{1j} - (2jn/N)\Delta a'_{1j} + C_{11}\Delta b'_{1j} + C_{12}\Delta b'_{2j} = 0 \\
&\Delta a''_{2j} + C_{21}\Delta a'_{1j} + C_{22}\Delta a'_{2j} + (2jn/N)\Delta b'_{2j} = 0 \\
&\Delta b''_{2j} + C_{21}\Delta b'_{1j} - (2jn/N)\Delta a'_{2j} + C_{22}\Delta b'_{2j} = 0
\end{aligned} \tag{17}
$$

式中 $n=1$; $N\geqslant 2$; $j=1, 2, \cdots, N$。

将上二个方程组用矩阵符号改写成

$$
[I]\begin{Bmatrix}\Delta a''_{10}\\ \Delta a''_{20}\end{Bmatrix} + \begin{pmatrix}C_{11} & C_{12}\\ C_{21} & C_{22}\end{pmatrix}\begin{Bmatrix}\Delta a'_{10}\\ \Delta a'_{20}\end{Bmatrix} = 0 \tag{18}
$$

$$
[I]\begin{Bmatrix}\Delta a''_{1j}\\ \Delta b''_{1j}\\ \Delta a''_{2j}\\ \Delta b''_{2j}\end{Bmatrix} + \begin{pmatrix}C_{11} & 2jn/N & C_{12} & 0\\ -2jn/N & C_{11} & 0 & C_{12}\\ C_{21} & 0 & C_{22} & 2jn/N\\ 0 & C_{21} & -2jn/N & C_{22}\end{pmatrix}\begin{Bmatrix}\Delta a'_{1j}\\ \Delta b'_{1j}\\ \Delta a'_{2j}\\ \Delta b'_{2j}\end{Bmatrix} = 0 \tag{19}
$$

解出这二个矩阵方程的特征值 (特征根)

$$
\lambda_{1,2} = \left[-(C_{11}+C_{22}) \pm \sqrt{(C_{11}-C_{22})^2 + 4C_{12}C_{21}}\right]/2 \tag{20}
$$

$$
\lambda_{1,2,3,4} = \left[-(C_{11}+C_{22}) \pm \sqrt{(C_{11}-C_{22})^2 + 4C_{12}C_{21}}\right]/2 \pm i(2jn/N) \tag{21}
$$

式中 $i=\sqrt{-1}$。显然, 如果这些特征根具有负实部, 则式 (7) 所表示的稳态响应轨迹便是稳定的。满足所有这些特征根有负实部的充要条件是

$$
C_{11}C_{22} - C_{12}C_{21} > 0 \tag{22}
$$

这就是稳态响应轨迹稳定与否的判据, 它只与油膜力的等效阻尼系数有关, 而与刚度无关。

五、算　　例

用本文的方法和用数值积分方法对一无定心弹簧刚性转子—SFDB系统进行计算, 所得结果见图 2、图 3 和附表。图 2 为典型的无量纲稳态响应轨迹, a 为用 4 阶 Runge-Kutta 法得到的结果, b 为用本文方法得到的结果。在用本文方法的计算中, 首先采用最速下降法求解方程组 (9) 式, 等找到合适的初值后再换用拟牛顿法迭代求解该方程组, 直待得到满意的精度。实践表明这样的算法非常有效, 对初值的要求不太高, 最后收敛也不慢。附表中列出了算得的部分等效动力系数和应用稳定性判据的结论。比较这些计算结果, 可见本文方法的精度与数值计算法的相当, 但计算机时则节省得多, 而且在物理上阐明了阻尼系数对稳定性的影响情况。

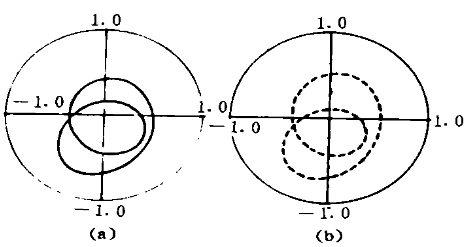

图 2　曲型无量纲稳态 1/2 阶次谐波响应轨迹

(W= 0.02, U= 0.2)

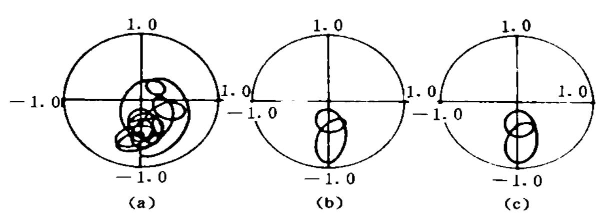

图 3　轴承参数对运动轨道稳定性的影响

(B= 0.05, W= 0.03, U= 0.4)

图 3a 是用 Runge-Kutta 法求出的小轴承参数时的不稳定情况。图 3b、3c 和附表表明用本文方法计算在 β< 0.005 时就没有稳定的次谐波响应。这说明用本文方法判断稳定性可能略

偏保守。实际系统中轴承参数总是大于 0.005 的。

表 1 算得的部分等效动力系数和应用稳定性判据的结论

动力系数	K_{11}	K_{12}	K_{22}	C_{11}	C_{12}	C_{22}	稳定否?
图 2 (b)	0.241	0.001	-.006	0.189	-.116	0.119	是
图 3 (b)	0.063	-.017	0.162	0.148	0.132	0.061	不
图 3 (c)	0.063	-.013	0.122	0.174	0.098	0.064	是

六、结　论

1. 在受不平衡谐和力激励的情况下，非线性油膜力作用处 (如本文中的轴承站) 的非同步稳态响应轨迹可通过该非线性系统运动微分方程的周期解求得。

2. 在非线性油膜力等效线性化模型的基础上，可求出等效线性系统的全部等效动力系数。它们与确定的运动轨道相对应，这一点与传统的概念不同。

3. 在微摄动理论基础上，本文提出了新的用于分析刚性转子—SFDB 系统非同步稳态响应稳定性的方法。计算精度与数值积分法的一致，计算机时则大大节省。而且通过建立等效线性化模型，能够揭示出一些非线性过程的物理本质。导出的稳定性判据只与等效阻尼系数有关，而与刚度无关。

4. 本文提供的是一解析方法，概念清晰，简便易用，当选择新参数时易于修改，且能使变更参数的效果迅速得到显示，因此对转子—SFDB 系统的设计工作特别有用。由于文中采用了迭代法求解代数方程组 (9) 式，所以只要以结构参数修改前的稳态响轨迹作为初始轨道，可以很快求出修改后的新的稳态响应轨迹，进而求出等效动力系统，立即判断出新轨迹的稳定性，这对于需要修改结构参数的设计工作，提供了很大方便。

5. 本文方法具有一般性，不仅适用于强迫振动非线性系统的次谐波共振情况 ($n=1$; $N\geqslant 2$; $j=1, 2, \cdots$)，也可推广用于谐波共振情况 ($n=N=1$; $j=1, 2, \cdots$)，主谐波共振情况 ($n=N=j=1$)[6]，超谐波共振情况 ($n\geqslant 2$, $N=1$, $j=1, 2, \cdots$) 和超次谐波共振情况 (n, $N\geqslant 2$; n/N, $N/n\neq 1, 2, \cdots$; $j=1, 2, \cdots$)。

参 考 文 献

[1] Booker, J. F., "A Table of the Journal-Bearing Integral", J. Basic Engrg, Vol. 87, pp. 533-535, 1964.

[2] Nikolajsen, J. L. and Holmes, R., "Investigation of Squeeze-Film Isolators for the Vibration Control of a Flexible Rotor", J. Mech. Engrg. Sci., Vol. 21, No. 4, pp. 247-252, 1979.

[3] 陈松淇、徐建康，"非线性元件次谐波运动的等效线性化"，航空动力学报，第 2 卷，第 2 期，117-120 页，1987 年。

[4] Tondl, A., "Notes on the Identification of Sub-harmonic Resonances of Rotors", J. Sound and Vibration, Vol. 31, No. 1, pp. 119-127, 1973.

[5] Licht, L., "The Dynamic Characteristics of a Turbo-rotor Simulation Supported on Gas-Lubricated Foil Bearings, Part 3", Trans. ASME, J. Lubrication Technology, Vol. 94, pp. 211-222, 1972.

[6] 张嘉欣、薛中擎，"刚性转子—挤压油膜阻尼器稳定性研究的新方法"，第四届全国振动理论及应用学术会议论文集下册，498-503 页，1990 年。

blades in the aeroengine to expand its range of stable operation.

ANALYTICAL METHOD FOR SUBSONIC CASCADE PROFILE

Liu Bo *(Northwestern Polytechnical University)*

ABSTRACT A method of subsonic cascade design for axial-flow compressor is provided as follows. The equations of continuity and quasi-irrotationality are transformed into the potential-stream function coordinates. Then a Laplace equation can be deduced for an aerodynamic parameter "Q". The boundary conditions thereby are given as the distributions of velocity coefficients on the stagnation streamlines of both suction and pressure sides of a flow channal. The flow field is obtained from the analytical solution of the Laplace equation. Subsequently the field is turned back into the physical plane by diffierentiation and integration. Then the blade profile coordinates and the geometry of the cascade result from this analysis. The method has an advantage over other inverse methods in the fact that the flow field parameter "Q" can be easily obtained from the analytical solution of the Laplace equation instead of the numerical solution of a complex diffierential equation. So the method is easy to be programmed and to save computing time. To illustrate the validity of the design method, two compressor stator blade profile with subsonic inlet Mach number were designed and compared with the method presented in ref. [3]. The good agreement between the two methods show the applicability of this method.

AN EXPERIMENTAL STUDY OF 3-D FLOW IN A CASCADE

Ji Chunjun, Zhu Zhuguo, Liu Qianzhi, Zhou Xinhai
(Northwestern Polytechnical University)

ABSTRACT An experimental investigation of three-dimensional flow in a cascade has been accomplished by means of flow visualization and detailed measurements, and also compared with the predictions of fully three-dimensional inviscid flow calculation. The experimental measurements of the three-dimensional flow in a highly cambered compressor cascade with nonplanar end wall reveal the distributions of flow parameters on blade surfaces and the whole flowfield in cascade channel. In comparison with the two-dimensional cascade measurements for the same blade section, the results show that the influence of the end wall shape changing on the flow is not confined to the vicinity of end walls, and can extend to the whole field when the aspect ratio of blading is small. The comparison between the experimental data and the computational results confirms that the inviscid flow calculation can predict the major features of three-dimensional flow in cascades. The flow visualization reveals the formation and development of vortex systems in the cascade passage, end wall and corner regions, which serve as a visualized information to understand the phenomena of complicated secondary flow in cascades. The experimental measurements provide a reliable basis to perfect the flow models, to investigate the mechanism of spanwise mixing in a cascade and to testify the capabilities of fully three-dimensional cascade flow calculation methods.

STABILITY ANALYSIS OF A RIGID ROTOR ON SFDB WITHOUT A CENTRALIZING SPRING

Zhang Jiaxin and Xue Zhongqing *(Northwestern Polytechnical University)*

ABSTRACT The stable nonsynchronous responses and the stability of motion of a rigid rotor supported on squeeze-film damper bearings (SFDB) without a centralizing spring are studied by means of harmonic balance method. The motion of the system is approximately simulated by two coupled

second-order differential equations. The stable nonsynchronous response at the action point of nonlinear oil film force can be obtained from the periodic solution of the differential equations of motion. With the help of an equivalent linearized model of the oil film force, the equivalent dynamic characteristic coefficients corresponding to the determined motion of the original system are obtained. A new method to analyse the stability of the motion of the equivalent linearized system is put forward in detail according to the theory of small pertubation. It is quite interesting to point out that the derived criterion for the motion stability is simple in form and depends on the equivalent damping coefficients only. A system with 1/2 order subharmonic response is taken as an example to illustrate this method. The calculated results are compared with those of fourth-order Runge-Kutta method. It is shown that our method has the same accuracy of calculation, but gains an advantage in saving computing time.

DYNAMIC ANALYSIS OF CENTRIFUGAL IMPELLER

Zhang Jin *(Beijing University of Aeronautics and Astronautics)*
Chen Xiangjun and Zang Jun *(Wuxi Aeroengine Research Institute)*
Wang Wenliang *(Fudan University)*

ABSTRACT A dynamic analysis technique is provided for rotating centrifugal impeller with guide blades and split blades. It is shown that multi-component partition can be made in repetitive sector region of the centrifugal impeller. The basic repetitive sector region of the centrifugal impeller is divided into three substructures: the guide blade, the split blade and the sectoral part of the disc. The Hermite generalized mass and stiffness matrices in the reduced coordinates are derived by successful combination of Benfield mode substitution transformation with group transformation. Therefrom the natural frequencies of the bladed disc coupled system are solved and the corresponding modal shapes are obtained from further transformation. The comparison between the analytical results obtained by using this and other methods and the experimental data verifies the reliability, practicability and considerable economic benefits of the method pressented in this paper.

ESTIMATION OF HIGH TEMPERATURE CREEP PARAMETERS FOR STRUCTURAL CERAMICS

Yang Xiaoguang, Ding Jun, Xong Changling
(Beijing University of Aeronautics and Astronaustics)

ABSTRACT Power-law high temperature creep parameters of structural ceramic materials are commonly deduced from load-point displacement data obtained form bend tests on the assumption that tensile and compressive behaviours obey the same constitutive law. However, it is now well recognized that this premise may not always be valid because of microcracking and cavitation. Meanwhile, former methods of creep parameters estimation are not suitable, due to a demand for many CPU time. Therefore, a new optimal estimation method is proposed for the structural ceramic creep parameters. Its governing equations are derived from non-coincidence of the neutral axis of a beam under bending with the cenctroids of the cross-sections, and from the creep response in terms of both curvature rate and load-point displacement rate as functions of the applied moment and creep parameters. Numerical solution of the governing equations is completed with golden section method. In order to obtain optimal estimation of the creep parament, a static optimal calculation program is used which turns the constrained minimum problem into an unconstrained minimum problem by penalty function. Then the problem is solved with variable matrix method that includes both DFP method and BFGS method. An example is given for a set